Electronic Supplementary Material (ESI) for Journal of Materials Chemistry A.

Supporting Information:

Electrodeposition of Ligand-Free Copper Nanoparticles from Aqueous Nanodroplets

Nicole E. Tarolla[a], Silvia Voci[a], Joshua Reyes-Morales[a], Andrew D. Pendergast[a], and Jeffrey E. Dick[a,b]*

[a]Department of Chemistry, The University of North Carolina at Chapel Hill, Chapel Hill, NC 27599, USA
[b]Lineberger Comprehensive Cancer Center, School of Medicine, The University of North Carolina at Chapel Hill, Chapel Hill, NC 27599, USA

*Corresponding Author: jedick@email.unc.edu

Table of Contents **Page**

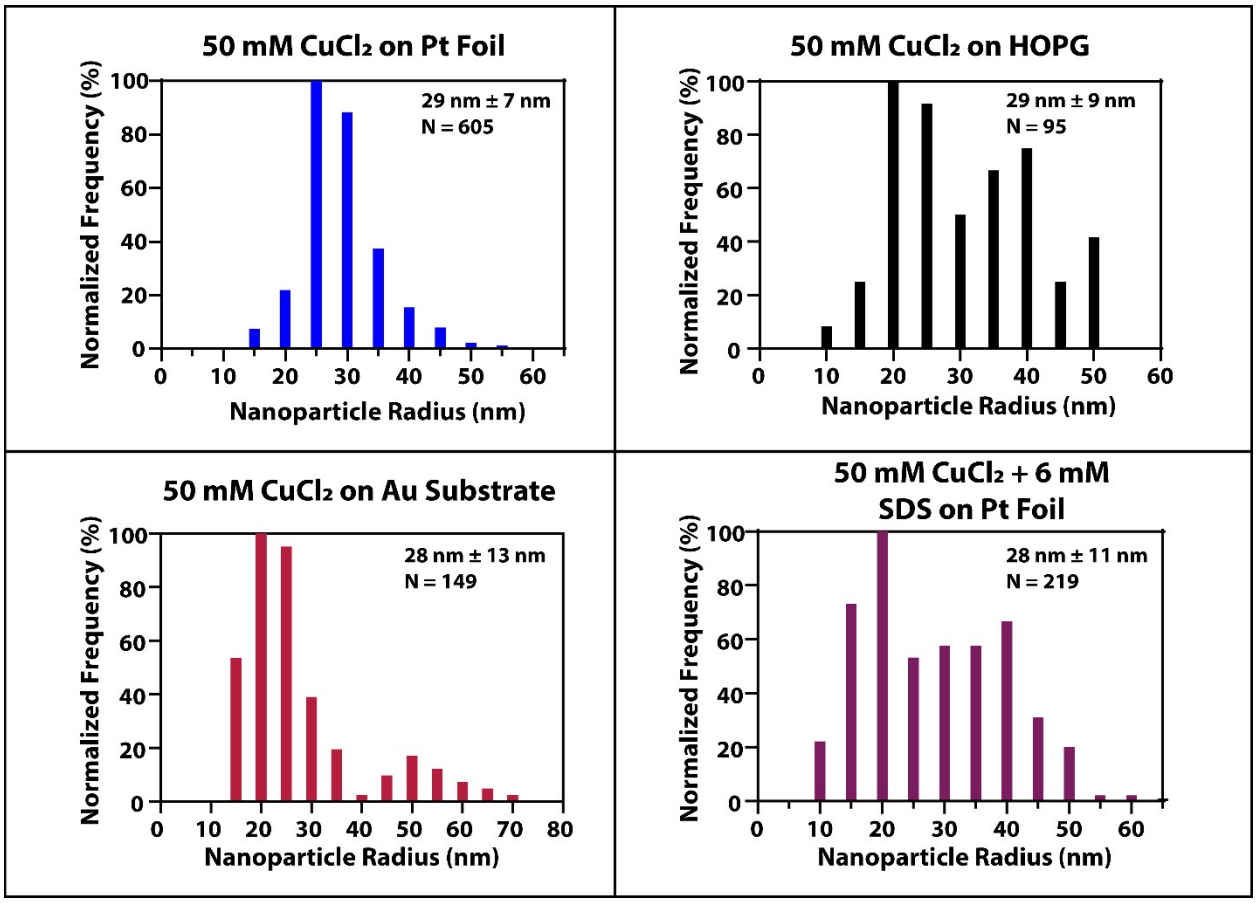

Figure S1. Histograms demonstrating the size distributions of copper nanoparticles deposited from aqueous nanodroplets composed of either 50 mM $CuCl_2$ or 50 mM $CuCl_2$ with 6 mM SDS on each of the different substrates, including their average radius, standard deviation, and sample size.

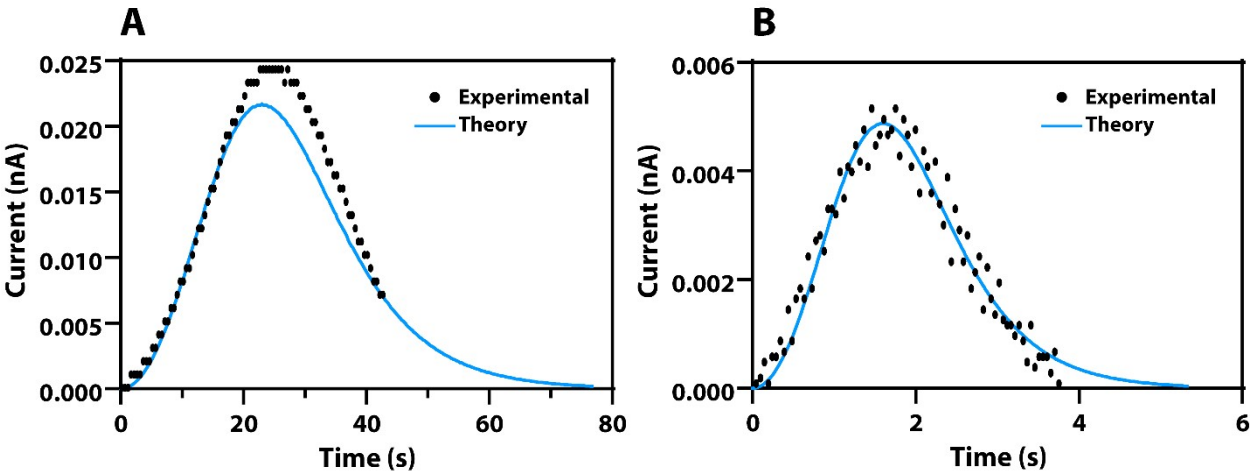

Figure S2. Theoretical Model vs Amperometric Results for Kinetics Analysis. Representative, experimentally obtained amperometric collision transients (black) overlaid with theoretical transients (blue), demonstrating electrokinetically limited growth. (A) Collision transient obtained using a Pt microelectrode (Pt UME, r ~ μm) at a potential of -0.30 V vs Ag/AgCl and (B) collision transient obtained using a Au microelectrode (Au UME, r ~ 6.25 μm) at a potential of -0.25 V vs Ag/AgCl. The emulsions were comprised of aqueous nanodroplets containing 50 mM $CuCl_2$ suspended in 0.1 M [TBA][PF_6] in 1,2-DCE with the complete amperometric i-t traces being performed for 200 seconds. Fixed parameters for the model include C = 0.05 M, Molar Volume = 7.09×10^{-6} m^3 /mol, and n = 2.

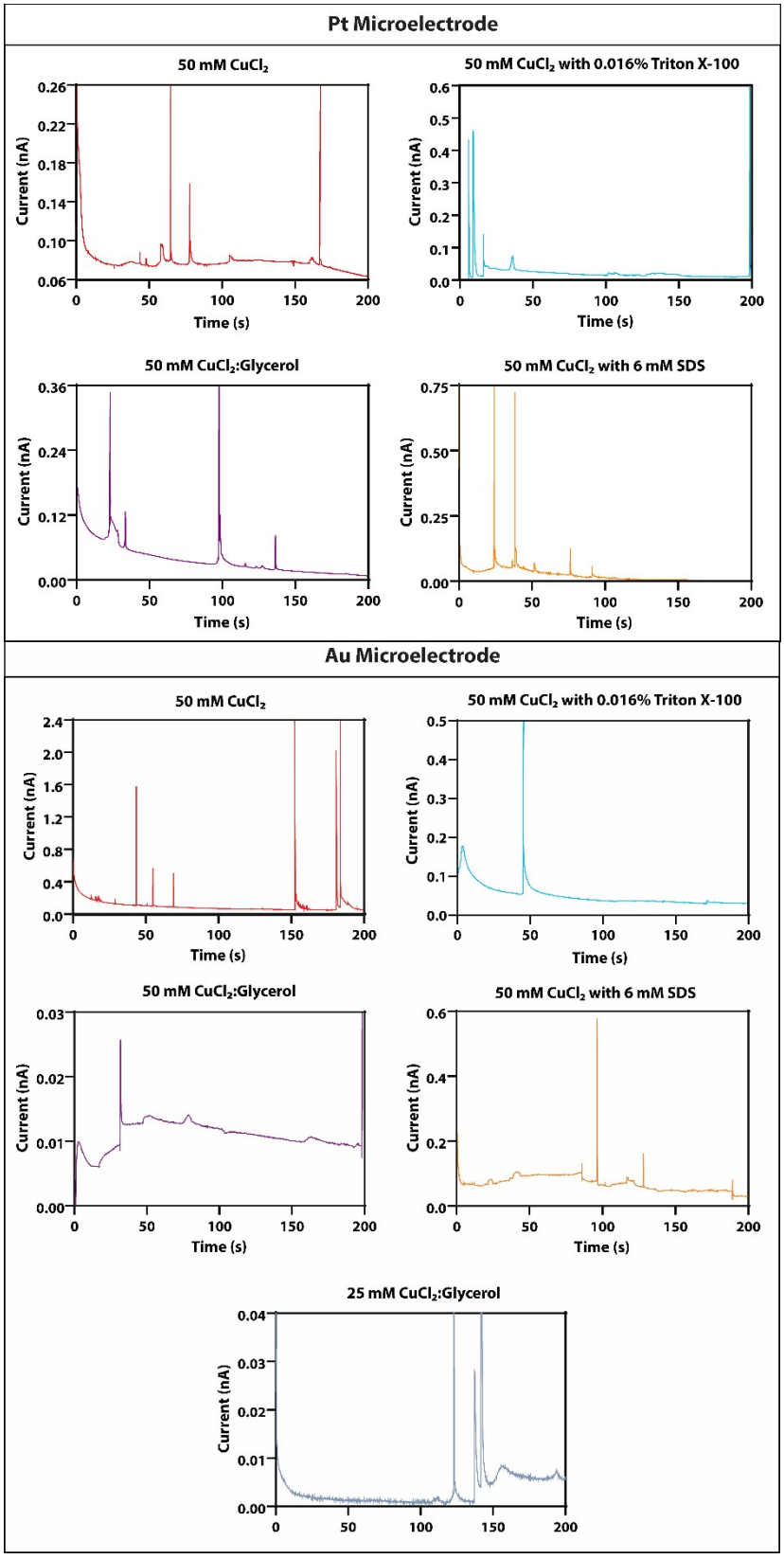

Figure S3. Representative amperograms of aqueous nanodroplets composed of various solution compositions suspended in 0.1 M [TBA][PF_6] in 1,2-DCE on a Pt microelectrode (r ~ 5 µm) or Au microelectrode (r ~ 6.25 µm) held at the potentials labeled in Table 1 in the main text.

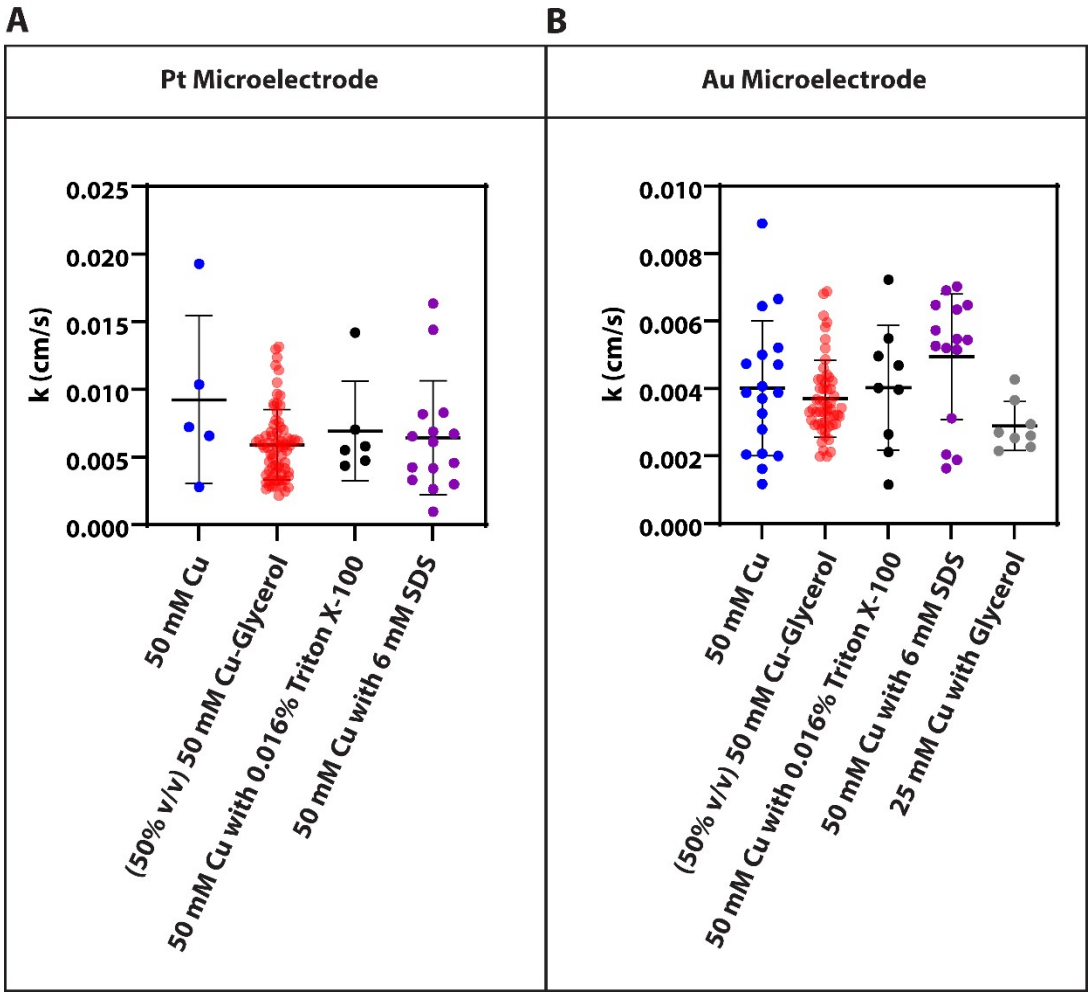

Figure S4. Summarized Kinetics Data. Plots of the calculated heterogenous rate constants, *k*, of a variety of 50 mM cupric chloride filled nanodroplet systems on a (A) Pt microelectrode (r ~ 5 μm) and (B) Au microelectrode (r ~ 6.25 μm), demonstrating the faster kinetics on platinum.

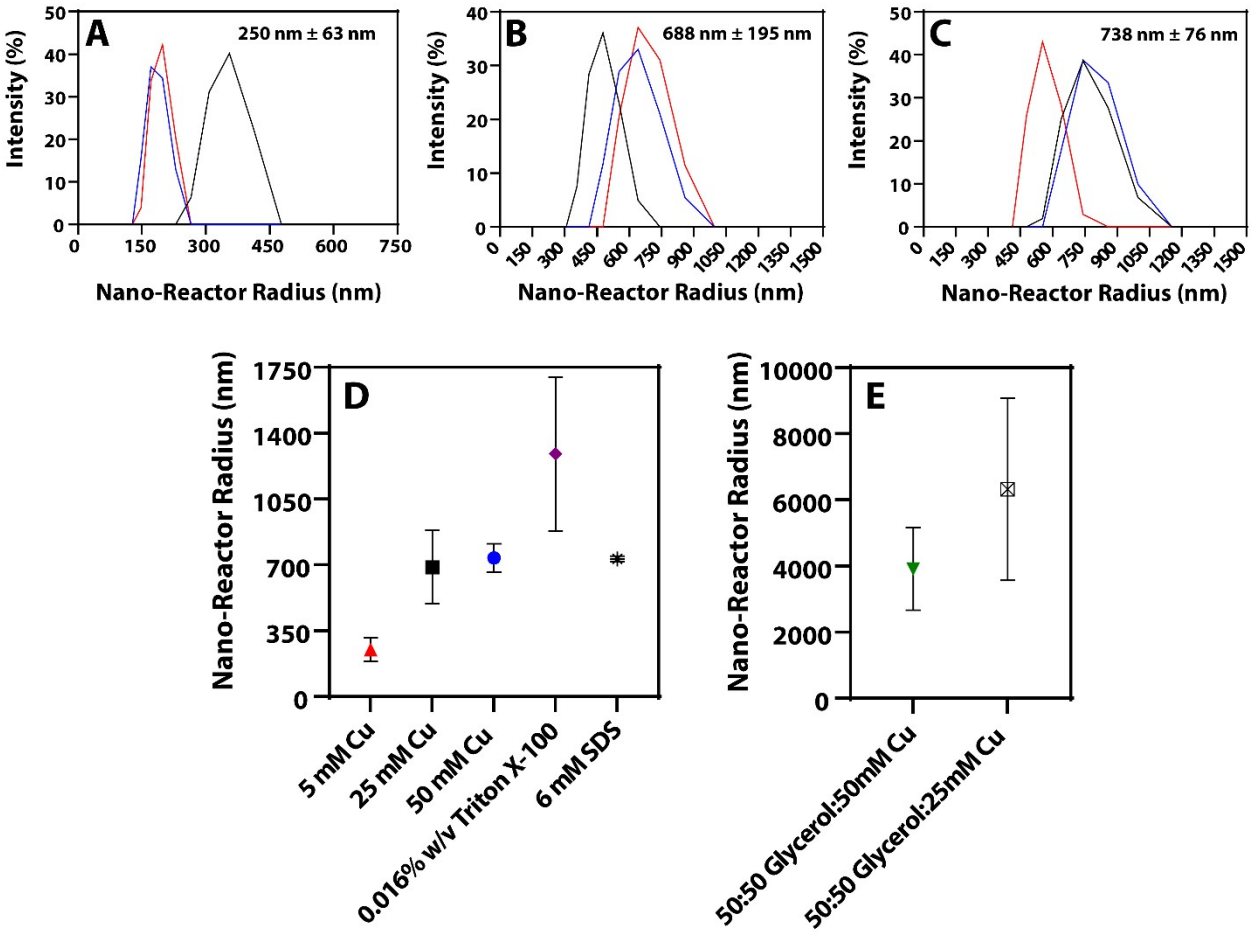

Figure S5. Dynamic Light Scattering (DLS) data of (A-C) 5 mM, 25 mM, and 50 mM $CuCl_2$ in 0.1 M [TBA][PF_6] in DCE, showing the size distribution of the droplets along with the calculated average and standard deviation. The black plot shows the first measurement, the blue shows the second, and the red shows the third. (D-E) DLS data showing the average radii and standard deviations for each of the solution variables tested. The DLS experiment was performed using 1 run with 3 measurements, each 60 seconds long, for the 5 mM, 25 mM, and 50 mM $CuCl_2$ data and 1 run with 3 measurements, each 120 seconds long, for the surfactant and glycerol trials. *Note that the glycerol containing solutions had a different nanodroplet to continuous phase ratio, resulting in larger nanodroplet radii.

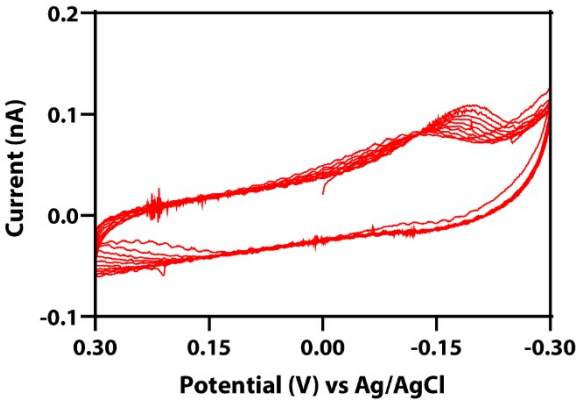

Figure S6. Cyclic voltammogram of reactors containing only water in 0.1 M [TBA][PF_6] in 1,2-DCE on a Pt UME (r ~ 5 μm) versus Ag/AgCl at a scan rate of 0.2 V/s, demonstrating some faradaic current due to oxygen reduction at sufficiently negative potentials, yet they are distinctly lacking the characteristic waves of deposition and stripping.

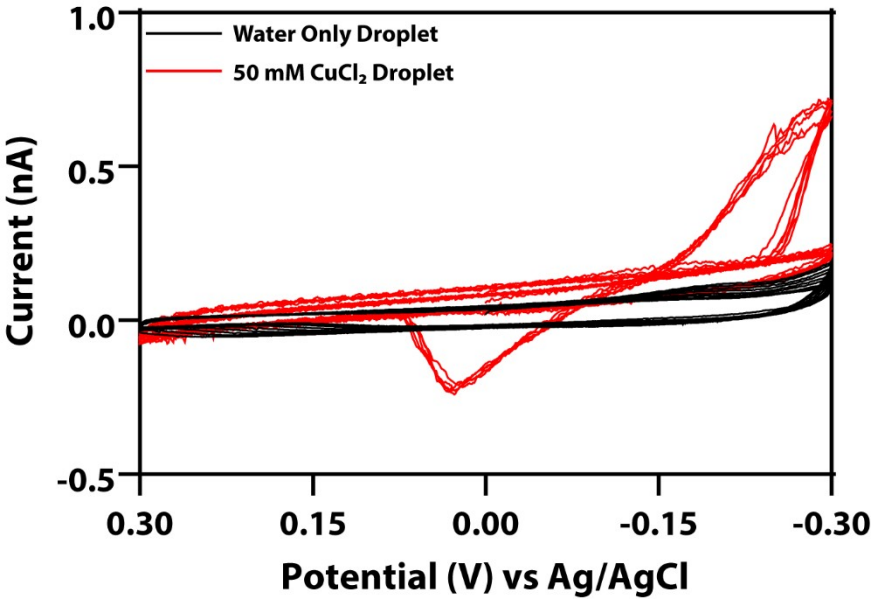

Figure S7. Overlaid cyclic voltammograms of a water only containing droplet (black) and a 50 mM $CuCl_2$ droplet (red) in 0.1 M [TBA][PF_6] in 1,2-DCE on a Pt UME (r ~ 5 µm) versus Ag/AgCl at a scan rate of 0.2 V/s. The electrodeposition wave and anodic stripping wave show great increases in current when compared to the cyclic voltammogram demonstrating a droplet containing only water.

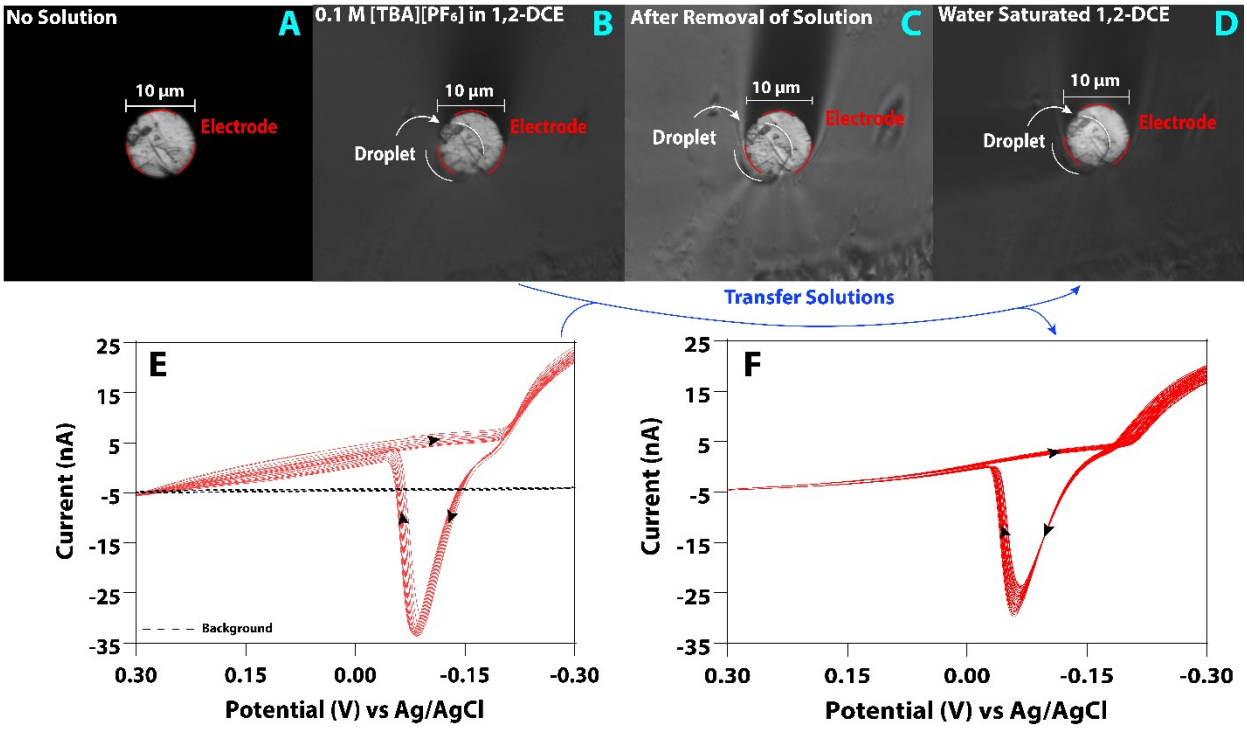

Figure S8. Correlated Electrochemical Experiments with Optical Microscopy. Correlated copper nanodroplet collision with optical microscopy using an exposure time of 7 ms and a magnification of 94.5x. (A) The Pt UME (microscopy determined r = 5.0 µm) before the emulsion has been added. (B) The single 50 mM $CuCl_2$ aqueous reactor (microscopy determined r = 4.4 µm) in 0.1 M [TBA][PF_6] in 1,2-DCE collided with the Pt UME (microscopy determined r = 5.0 µm). (C) The single 50 mM $CuCl_2$ aqueous reactor stable on the Pt UME (microscopy determined r = 5.0 µm) after removal of the emulsion. (D) The single 50 mM $CuCl_2$ aqueous reactor (microscopy determined r = 4.4 µm) in water saturated 1,2-DCE attached to the Pt UME (microscopy determined r = 5.0 µm). (E) Cyclic voltammogram showing the electrodeposition and anodic stripping of the single 50 mM $CuCl_2$ reactor in 0.1 M [TBA][PF_6] in 1,2-DCE on a Pt UME (microscopy determined r = 5.0 µm) versus Ag/AgCl at a scan rate of 0.2 V/s. (F) Cyclic voltammogram after the transfer of the single 50 mM $CuCl_2$ reactor to water saturated 1,2-DCE on a Pt UME (microscopy determined r = 5.0 µm) versus Ag/AgCl at a scan rate of 0.2 V/s.

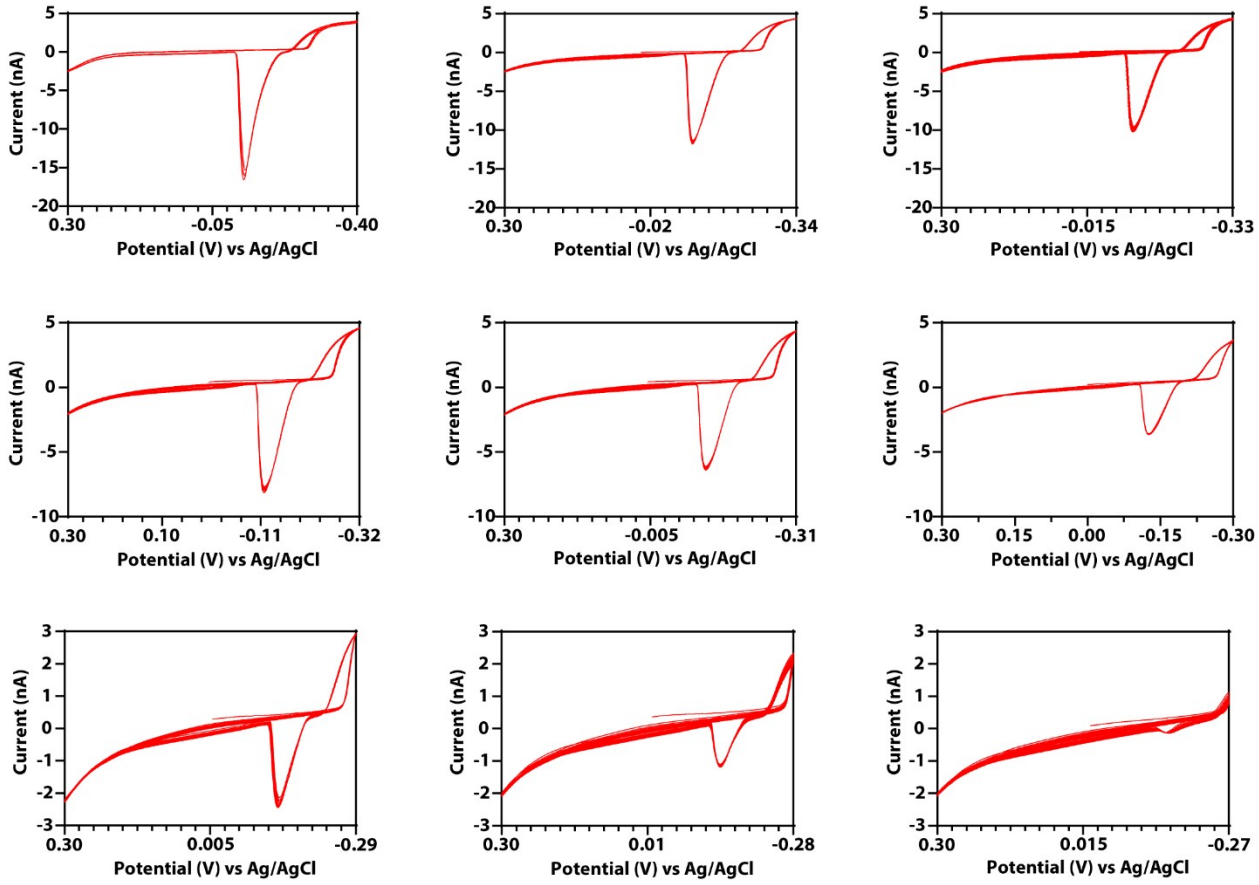

Figure S9. Cyclic voltammograms of a collection of reactors, instead of a single nanodroplet consisting of 50 mM $CuCl_2$ in a solution of water saturated 1,2-DCE on a Pt UME (r ~ 5 µm) versus Ag/AgCl at a scan rate of 0.025 V/s with switching potentials ranging from -0.40 V to -0.27 V. The voltammogram at a switching potential of -0.40 V gives an average charge of 27,500 pC while the voltammogram at a switching potential of -0.27 V results in an average charge of 303 pC. As seen above, the trend is still observed that more positive switching potentials result in a decrease in the charge passed for the stripping peak.

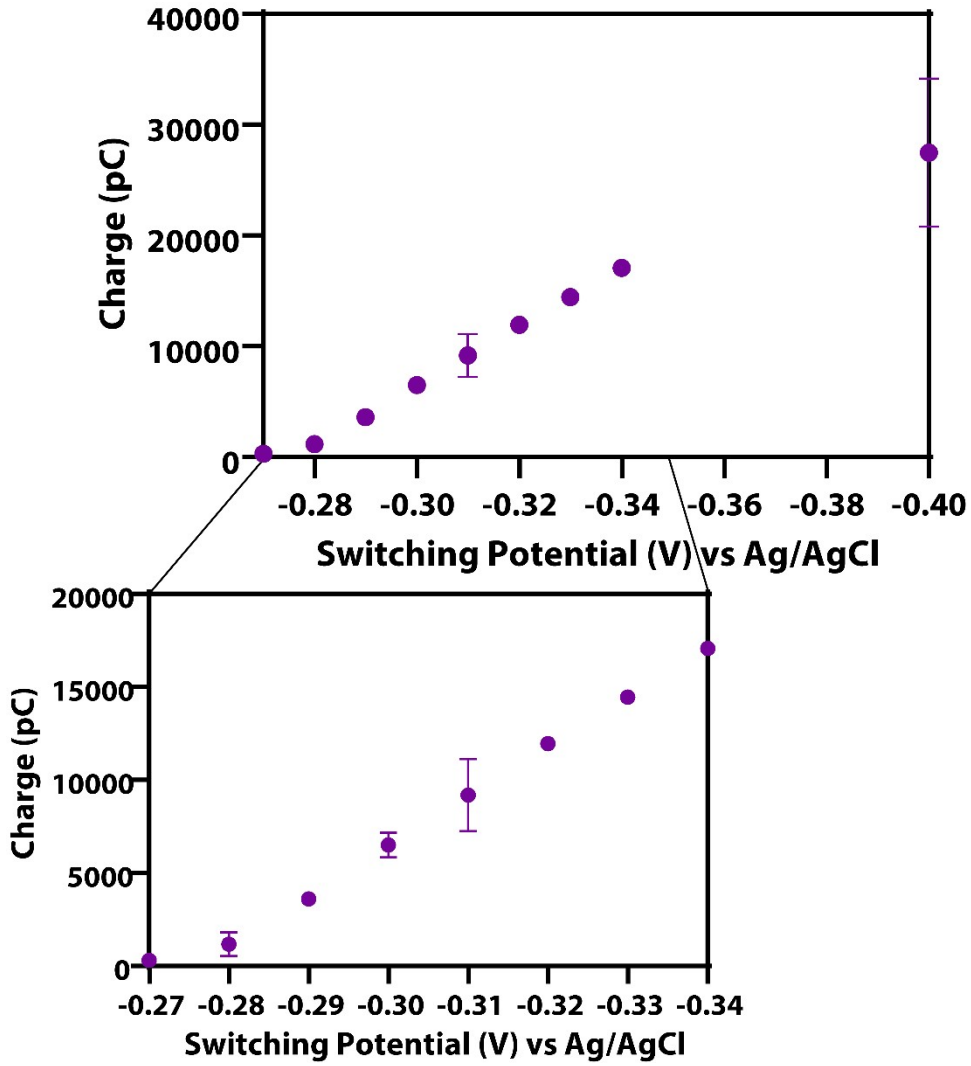

Figure S10. Overall trend of the integrated charge of the stripping peak as a function of switching potential from the data in Figure S9 using a scan rate of 0.025 V/s. The trend shows an increase in the oxidative stripping peak's charge as the switching potential is made negative from -0.27 V to -0.34 V with a switch in potential every 10 mV to finally -0.40 V, which was used to get data on the initial nanodroplet size.

Materials and Methods

Reagents and Materials

Tetrabutylammonium hexafluorophosphate ([TBA][PF_6], 99%), copper(II) chloride dihydrate ($CuCl_2 \cdot 2H_2O$, 99.95%), glycerol (99%), Triton X-100, and sodium dodecyl sulfate (SDS, 99%) were purchased from Sigma-Aldrich. 1,2-dichloroethane (1,2-DCE, 99.9%) and nitric acid (HNO_3, TraceMetal™ Grade) were purchased from Fisher Scientific. All reagents were used as received. Stock solutions of copper(II) chloride dihydrate were made in nanopore water (18.2 MΩ, Thermo), stored in a dark refrigerator (4 °C) to avoid photodecomposition, and diluted as needed to be used in emulsion preparation. Platinum microelectrode (Pt UME, r ~ 5 μm), gold microelectrode (Au UME, r ~ 6.25 μm), and Ag/AgCl reference electrode were purchased from CH Instruments (Austin, TX). The platinum foil substrate (0.05 mm thick, 99.9%) was obtained from Sigma-Aldrich.

Instrumentation

All electrodeposition experiments were performed using a CHI model 601E potentiostat (CH Instruments, Austin, TX) on the "cyclic voltammetry" mode in a grounded Faraday cage except for the 25 mM $CuCl_2$:Glycerol (50%, v/v). Those experiments were performed on a Pine Research AFTP5 WavePico Wireless unit in the "cyclic voltammetry" mode using Pine Research Aftermath Software (Durham, NC). An unpolished glassy carbon rod and a salt bridge (containing 3% w/v agarose) connecting the emulsion and the Ag/AgCl reference electrode (1 M KCl) were used as the counter and reference electrodes. The potential was cycled between +0.30 and -0.30 V vs. Ag/AgCl at a scan rate of 0.2 V/s. For the single nanodroplet experiments, a range of switching potentials were used at a scan rate of 0.025 V/s. The emulsion was prepared using a Q500 ultrasonic processor (Qsonica, Newtown, CT) with a microtip probe. Growth kinetics analysis was performed using MATLAB version R2019b. Dynamic light scattering studies used a Zetasizer Nano ZS (Malvern, Westborough, MA) and quartz cuvette. Scanning electron microscopy (SEM) images were taken using a Helios 600 Nanolab dual beam system (FEI, Hillsboro, OR) at 20 kV to 25 kV and 0.17 nA to 1.4 nA. Energy dispersive spectroscopy (EDX) spectra were obtained using a Hitachi S-4700 Cold Cathode Field Emission Scanning Electron Microscope and INCA PentaFET-x3 (Oxford, Abingdon, UK) system at 20 kV or Helios 600 Nanolab dual beam system

(FEI, Hillsboro, OR) at 20 kV to 25 kV and 0.17 nA to 1.4 nA. Transmission Electron Microscopy (TEM), Energy Dispersive Spectroscopy, and Selected Area Electron Diffraction were performed on a Thermo Scientific Talos F200X at 200 kV.

General Nanodroplet Mediated Electrodeposition Procedure

The water in oil emulsion was prepared in a similar manner to a previously reported method.[1,2] Firstly, an aliquot of an aqueous solution containing $CuCl_2 \cdot 2H_2O$ was prepared in a 20 mL glass scintillation vial before an aliquot of 1,2-DCE containing 0.1 M [TBA][PF_6] was added. The solution was then subjected to ultrasonication at a pulse amplitude of 40% and a pulse method of 5 s on and 5 s off to form the emulsion. The microelectrode was cleaned by polishing on a 0.05 and 0.30 μm alumina powder polishing pad and stored in 200 mM nitric acid. For TEM analysis, nanoparticles were made from the aforementioned solutions with the following specific differences: A TEM grid (pure carbon 400 mesh titanium) was placed into the emulsion solution, and an electrical contact was made using stainless steel tweezers.

Single Reactor Isolation Procedure

The water in oil emulsion was prepared as stated above. The water saturated 1,2-DCE was made by mixing 2 mL of nanopore water (18.2 MΩ, Thermo) with 50 mL of the 1,2-DCE solution, letting it sit overnight, and then extracting the 1,2-DCE layer. A 50 mM $CuCl_2$ droplet was electrodeposited on the Pt UME by cycling through potentials of +0.30 and -0.30 V vs. Ag/AgCl at a scan rate of 0.2 V/s and stopping the scan when a reductive electrodeposition peak was observed. The Pt UME was then transferred to the solution of water saturated 1,2-DCE and cyclic voltammetry experiments proceeded at a scan rate of 0.025 V/s and a variety of switching potentials.

Growth Kinetics and General Amperometry Procedure

The water in oil emulsion was prepared as stated above with 25 μL of the 50 mM $CuCl_2$ containing solutions in 5 mL of 0.1 M [TBA][PF_6] in 1,2-DCE for all solutions, except glycerol-containing emulsions, then sonicated. The 50 mM $CuCl_2$:Glycerol (50%, v/v) emulsion was prepared using a ratio of 25 μL of aqueous nanodroplets in 4 mL of the continuous phase and the 25 mM $CuCl_2$:Glycerol (50%, v/v) emulsion was prepared using a ratio of 50 μL aqueous nanodroplets in

5 mL of the continuous phase. In order to observe reproduceable collision transients, these ratios were used. The concentrations of surfactants in solution were made under their critical micelle concentration. A platinum UME (r ~ 5 μm), glassy carbon counter, and Ag/AgCl reference electrode (connected via a 3% w/v agarose in 1 M KCl salt bridge) were placed in the emulsion and held at the respective potentials shown in Table 1 vs. Ag/AgCl for 200 seconds at a 0.05 second sampling interval.

Deposition Procedure for SEM

The platinum foil was initially cleaned by submersion in 200 mM nitric acid overnight and then rinsed with water, ethanol, and acetone. The gold piece was cleaned by submersion into 600 mM nitric acid overnight, sonicated in water for 3 minutes, dipped into piranha to remove any carbon contaminants, sonicated in water and then ethanol for 3 minutes each, before finally being rinsed in acetone.

For the 50 mM $CuCl_2$ nanoparticles on platinum foil: The water in oil emulsion was prepared as stated above by sonicating 25 μL of 50 mM $CuCl_2$ in 5 mL of 0.1 M [TBA][PF_6] in 1,2-DCE. The platinum foil was submerged in the emulsion and held at a potential of -0.40 V vs. Ag/AgCl for 350 seconds at a 0.05 second sampling interval. It was then cleaned by being submerged in acetone for 10 minutes, ethanol for 20 minutes, and then rinsed with acetone before being imaged.

For the 50 mM $CuCl_2$ nanoparticles on gold: The water in oil emulsion was prepared as stated above by sonicating 25 μL of 50 mM $CuCl_2$ in 5 mL of 0.1 M [TBA][PF_6] in 1,2-DCE. The potential was held at -0.40 V for 250 seconds.

For the 50 mM $CuCl_2$ nanoparticles on HOPG: The water in oil emulsion was prepared as stated above by sonicating 25 μL of 50 mM $CuCl_2$ in 5 mL of 0.1 M [TBA][PF_6] in 1,2-DCE. The potential was held at -0.80 V for 40 seconds.

For the 50 mM $CuCl_2$ with 0.016% Triton X-100 nanoparticles on Pt Foil: The water in oil emulsion was prepared as stated above by sonicating 25 μL of 50 mM $CuCl_2$ with 0.016% Triton X-100 in 5 mL of 0.1 M [TBA][PF_6] in 1,2-DCE. The potential was held at -0.15 V for 1000 seconds. The deposition potential was chosen for consistency to the one used in the kinetics analysis.

For the 50 mM $CuCl_2$ with 6 mM SDS nanoparticles on Pt Foil: The water in oil emulsion was prepared as stated above by sonicating 25 µL of 50 mM $CuCl_2$ with 6 mM SDS in 5 mL of 0.1 M [TBA][PF_6] in 1,2-DCE. The potential was held at -0.23 V for 200 seconds. The deposition potential was chosen for consistency to the one used in the kinetics analysis.
ImageJ measurement tools were used to determine nanoparticle size.

Correlated Microscopy Instrumentation and Procedure

The water in oil emulsion was prepared as stated previously but with a higher droplet concentration of 75 µL of 50 mM $CuCl_2$ in 5 mL of 0.1 M [TBA][PF_6] in 1,2-DCE.
The correlated microscopy system for the imaging of collisions of aqueous nanodroplets filled with 50 mM $CuCl_2$ was composed by a Leica DMi8 microscope (Leica Microsystems, Germany) equipped with a Lambda LS xenon arc lamp (Sutter Instrument Company, Novato, CA), a Leica CTR advanced electronics box (Leica Microsystems, Germany), a Leica SP box LMT200 (Leica Microsystems, Germany), a Complementary Metal-Oxide Semiconductor camera (C-MOS C13440 from Hamamatsu, Hamamatsu Japan), a Lambda SC SmartShutter controller (Sutter Instrument Company, Novato, CA), two Lambda VF-5 tunable filter changers (Sutter Instrument Company, Novato, CA) and a Lambda 10-3 optical filter changer and SmartShutter control system (Sutter Instrument Company, Novato, CA). A stepper and piezo positioner/controller (CH Instruments, Inc., Auston, TX) was placed on top of the microscope stage. The positioner/controller was mobilized by a 920D bipotentiostat (CH Instruments, Inc., Austin, TX). Pt SECM tip electrodes (5 µm radius) and Ag/AgCl/KCl 1 M electrodes were used respectively as working and reference electrodes and purchased from CH Instruments, while a glassy carbon rod was used as counter electrode. For microscopic imaging in combination with electrochemical analysis, an inverted 94.5× microscope objective from Leica (94.5×/1.4, 0.14 mm) was used and cyclic voltammetry was performed using a scan rate of 0.2 V/s from +0.30 V to -0.30 V vs Ag/AgCl. Optical images in bright-field mode (exposure time of 7 ms) were simultaneously recorded with the electrochemical signal resulting from the collision of a water nanodroplet with the electrode surface.

Simulation Specifications

The dynamics of nanoparticle growth and dissolution within single aqueous nanodroplets were interrogated through finite element modelling using COMSOL Multiphysics 5.5 with the Electrodeposition Module. For the two-electron electrodeposition of $CuCl_2$ to zero valent Cu(s), analyte flux was modelled using Butler-Volmer kinetics with an exchange current density of 50 mA/cm^2. The electrode potential was controlled with a time-dependent interpolation triangle-wave function to match standard cyclic voltammetry behavior. The electrodeposition reaction was simulated under conditions of excess supporting electrolyte with minimal solution resistance using the Electroanalysis charge conservation model within COMSOL. Cu^{2+} reduction and Cu^0 oxidation were limited to the boundary of the deposited hemispherical nanoparticle, generating a single nanostructure within each droplet. The physical growth or dissolution of the nanoparticle was controlled using the coupled Tertiary Current Distribution and Deformed Geometry interfaces to relate Cu^{2+} flux at the nanoparticle surface to the thickness of an electrodeposited layer. All simulated potentials are normalized to the arbitrary formal potential of the $Cu^{2+}/Cu(s)$ couple (i.e., $E^0 = 0$ V). A time dependent solver configuration with a primary current distribution initialization was used for all simulations with automatic remeshing based on minimum mesh element quality. Simulations were performed using a computer equipped with an Intel Core i5-8400 CPU (2.80 GHz) and 8 GB of RAM.

To probe methods of voltammetric control, the electrodeposition of a single Cu nanoparticle was simulated inside a single aqueous nanodroplet using a 2D-axissymetric geometric interface. The electrodeposition domain was modelled as a 1.3 μm radius aqueous droplet containing 50 mM $CuCl_2$ with an electrode-droplet contact radius of 150 nm. To control hemispherical growth, the initial electroactive surface was limited to a hemisphere with radius 0.2 nm centered at the axis of symmetry. The dissolving-depositing species at the hemisphere copper electrode was modelled as a face-centered cubic (FCC) packed solid copper with a

density of 8.96 g/cm^3 and a molar mass of 63.55 g/mol. The dynamic nanoparticle geometry during the electrodeposition was simulated using the coupled Deformed Geometry and Tertiary Current Distribution Multiphysics interfaces. The hemispherical nanoparticle boundary was thus controlled by the thickness of the deposited Cu phase calculated directly from the Cu^{2+} flux to the hemisphere nanoparticle electrode. All other geometric boundaries were held constant using the zero normal displacement boundary condition within the coupled Multiphysics interface. Additional simulation details are available upon request.

Relevant Simulation Parameters

Table 1 | Representative COMSOL Simulation Parameters. Physical and chemical parameters for Cu nanoparticle deposition simulations by cyclic voltammetry and amperometry.

Parameter	Value	Units	Description
D_Cu	$5 \cdot 10^{-6}$	[cm^2/s]	Diffusion coefficient of Cu^{2+} species
C_Cu	50	[mol/m^3]	Concentration of Cu^{2+} species
Eformal	0	[V]	Formal potential (relative) for Cu^{2+}/Cu^0
v	0.025 to 0.2	[V/s]	CV Scan Rate
Ei	0	[V]	Initial potential for CV scan
Ef	-0.18 to -0.28	[V]	Switching potential for CV scan
ts	Abs(Ei-Ef)/v	[s]	Length of individual CV scan segment
rContact	150	[nm]	Droplet-Electrode contact radius
RDrop	1.3	[µm]	Droplet radius
EAppl	-0.18 to -0.28	[V]	Amperometric pulse potential
tPulse	60	[s]	Amperometric pulse duration

Table 2 | Simulated CV Potential Waveform Interpolation Function. Linear interpolation function for two-segment potential scan during simulated CV depositions.

Time (t)	ET(t)
0	Ei
ts	Ef
2*ts	Ei

Extended Simulation Discussion

The potential-controlled synthesis of single Cu nanoparticles using cyclic voltammetry was simulated at a range of potential sweep conditions to probe the effects of the potential waveform on resultant nanoparticle size within the domain of a single aqueous nanodroplet. Under a classical amperometric electrodeposition, a constant potential is applied to the electrode surface at some overpotential, η, above the formal potential, E_{formal}, for the redox couple over some duration, τ. At sufficient overpotentials and sufficiently long deposition times, the contents of a single nanodroplet will be completely electrolyzed which will generate a nanoparticle with dimensions governed by the size of the nanodroplet reactor and the concentration of precursor in the droplet. Under incomplete electrolysis, the size of a resultant nanoparticle can be controlled by the applied potential or the deposition timeframe as illustrated in Figure S11. At increasing overpotentials, the metal salt contents of the nanodroplet are rapidly consumed, resulting in a sharp amperometric blip response and thus steep nanoparticle growth. By reducing this overpotential, the slope of the nanoparticle growth curve can be flattened with a correlated broadening of the amperometric response, however, relatively mild overpotentials can still completely consume droplet contents over seconds. By modulating the pulse duration, as illustrated in Figure S11C, a nanoparticle of a prescribed size can be generated. However, during typical nanodroplet mediated electrodeposition, it is difficult to control the duration of the applied potential pulse following collision. Therefore, an electrochemical method that is independent of the moment of collision offers a distinct advantage in generating nanoparticles of a prescribed size during a collision experiment.

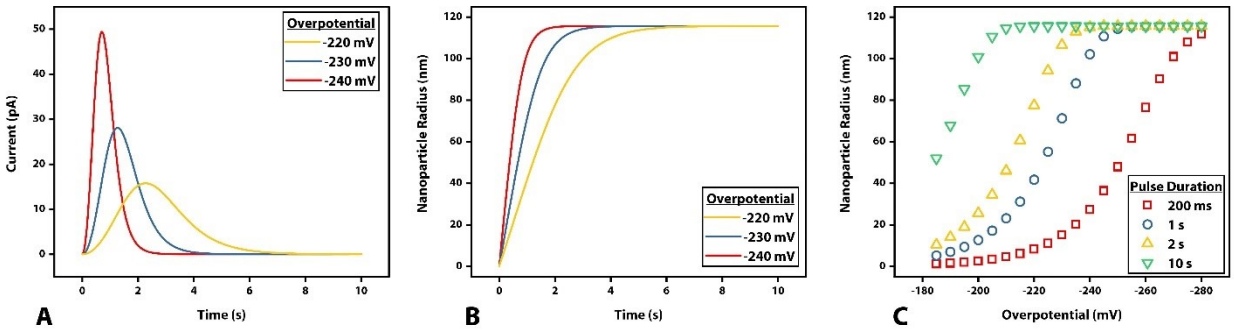

Figure S11 | Simulated Amperometric Electrodeposition in Aqueous Nanodroplets. A) Simulated i-t traces for the electrodeposition of 50 mM Cu^{2+} within a 1.3 µm radius nanodroplet at a range of overpotentials corresponding to complete electrolysis of reactor contents in under ten seconds. B) Simulated growth curves for representative i-t traces presented in A, corresponding to the nucleation of a 115 nm radius hemispherical Cu nanoparticle at different rates modulated by the applied potential. C) Simulated nanoparticle size at a range of overpotentials from -185 to -280 mV following amperometric pulse durations of 200 ms (red), 1 s (blue), 2 s (yellow), and 10 s (green), demonstrating the need for precise temporal control to modulate electrodeposited nanoparticle size within aqueous nanodroplets.

For a reversible system, such as that of an electrodeposited copper nanoparticle, cyclic voltammetry provides a facile method to repeatedly probe a single reactor *in situ* by alternating between regimes of nanoparticle growth by reduction and nanoparticle stripping by oxidation, independent of the moment of collision. This electrochemical diagnostic characterization of a single nanodroplet can be achieved rapidly to reveal thermodynamic and kinetic data for heterogeneous populations droplet-by-droplet. From the triangle waveform conventionally used within cyclic voltammetry, the switching potential (E_{switch}) can be tuned to exact control regarding the potential applied above the formal potential and the timeframe during which deposition occurs. Therefore, the overpotential-time profile for a nanoparticle electrodeposition under cyclic voltammetry control is dependent not only on the switching potential, but also the scan rate. At potentials negative relative to the formal potential, the nanoparticle experiences kinetic limited growth, transitioning to a mass-transfer limited regime at sufficiently cathodic potentials. By modulating the switching potential, the timeframe in each of these domains and the maximum applied potential can be tuned to direct either complete or partial electrolysis of the precursor ion to a solid nanoparticle, thereby directly controlling nanoparticle size. Alternatively, the growth of a single nanoparticle under voltammetric conditions can be controlled by directly changing the scan rate. For a given switching potential, a slower scan rate will extend the time during which electrodeposition can occur, thereby manifesting in larger

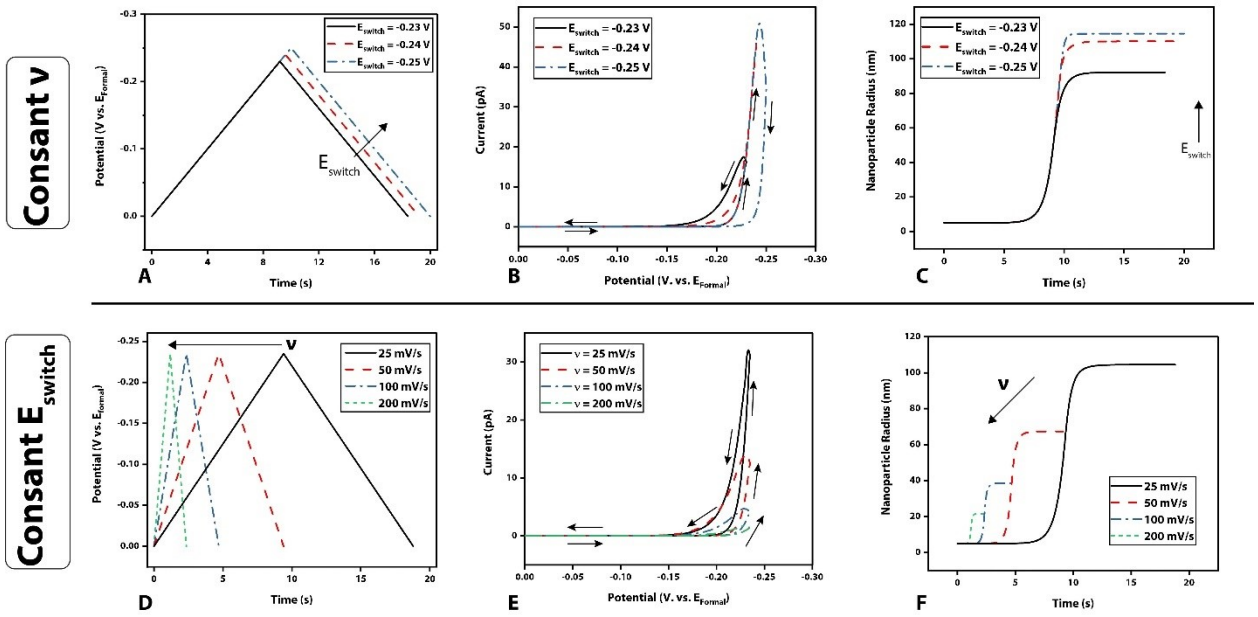

Figure S12 | Simulated Voltammetric Electrodeposition in Aqueous Nanodroplets. A) Representative potential-time profiles for simulated electrodepositions under voltammetric control with a variable switching potential. B) Representative simulated CV data at different switching potentials, demonstrating unique voltammetric profiles at a constant scan rate. C) Simulated nanoparticle growth curves for a range of switching potentials, demonstrating significant control in nanoparticle size as a function of CV parameters. D) Representative potential-time profiles for simulated electrodepositions under voltammetric control with a scan rate. E) Simulated CV data at a range of scan rates with a constant switching potential, illustrating the convolution of deposition time and deposition potential during voltammetric electrodeposition within single droplets. F) Simulated nanoparticle growth curves for a constant switching potential at a range of scan rates, demonstrating further size control through voltammetry.

nanoparticles. The effects of modulating the switching potential and scan rate are illustrated below in Figure S12, demonstrating dynamic control of resultant nanoparticle sizes by voltammetry.

From these electrodeposition simulations, a number of voltammetric responses can be observed which provides insight regarding nanoparticle growth directly from voltammetric shape. Under voltammetric conditions, the current response at the dynamic nanoparticle electrode surface is convoluted between the applied potential, nanoparticle size, and analyte flux. By probing the i-E traces under a range of scan rates and switching potentials, voltammetric peaks including nucleation loops, gaussian peaks, and mixed peaks can be resolved as presented in Figure S13. For this range of voltammetric responses, the general shape of the peak can be qualitatively related to the extent of electrolysis within the droplet, manifesting as complete electrolysis for gaussian-type peaks and some degree of incomplete electrolysis for other peak shapes. Currently, these voltammetric features are inaccessible during experimentation due to the convolution of oxygen reduction, however, we are currently exploring nanodroplet mediated

electrodeposition under non-ambient conditions to decouple the current contributions of nanoparticle growth and background voltammetric processes.

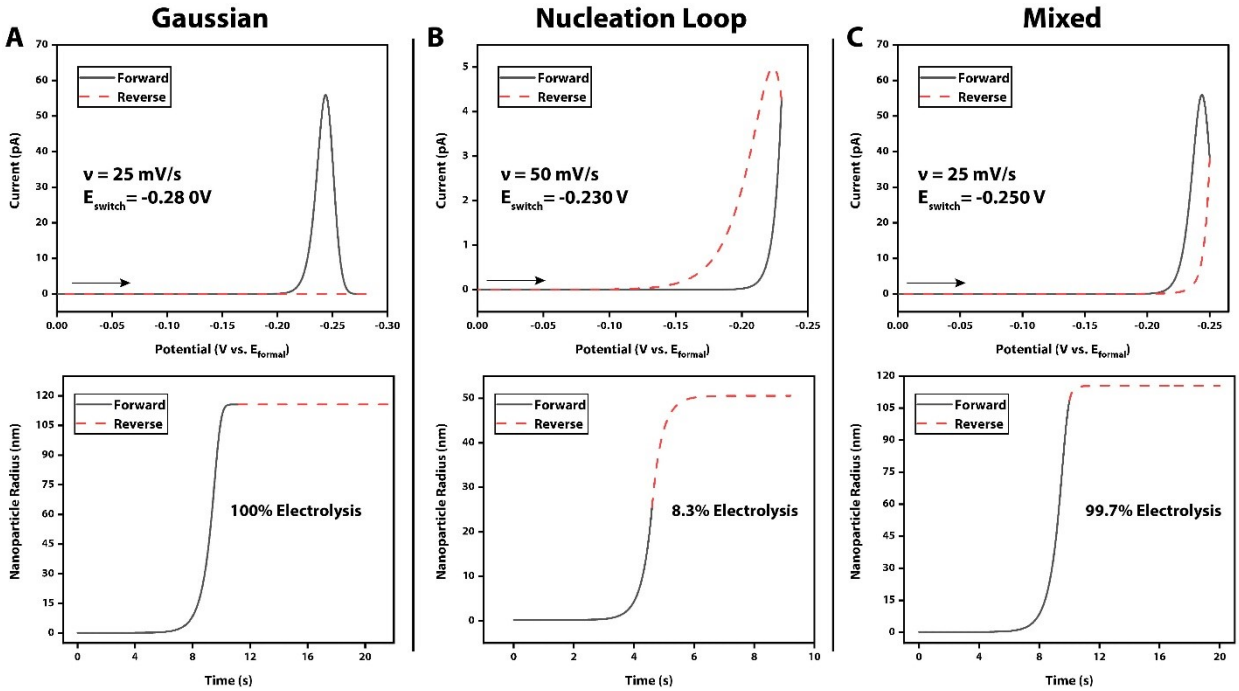

Figure S13 | Probing the Voltammetric Response in Single Reactors. A) Representative gaussian-type voltammetric peak and corresponding nanoparticle growth curve, revealing complete electrolysis during the forward scan and negligible current during the reverse voltammetric scan. B) Representative CV response of a nucleation-loop type response with corresponding nanoparticle growth curve, revealing incomplete electrolysis during voltammetric cycling. C) Representative mixed-type response with incomplete electrolysis during the forward scan and continued electrodeposition on reverse scan to near-complete electrolysis.

Simulation Geometry

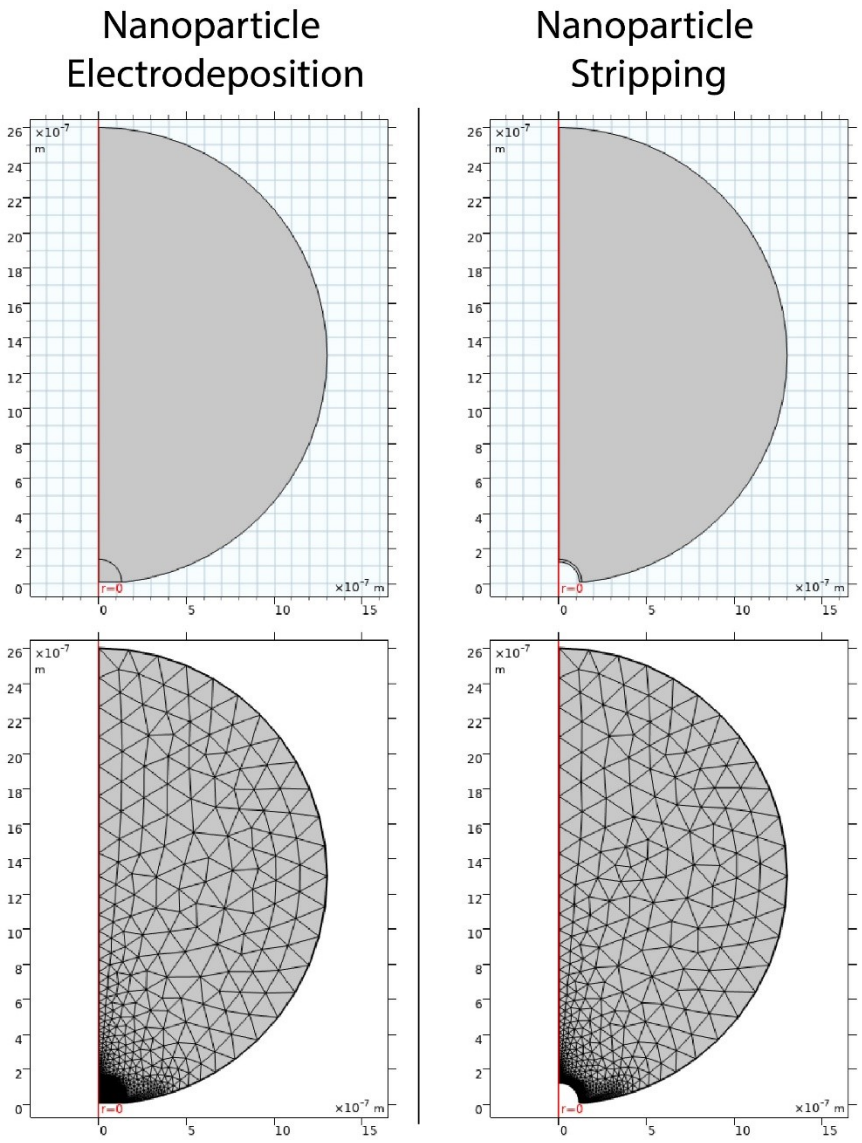

Figure S14 | COMSOL Finite Element Modelling Simulation Geometry. Representative simulation geometries and manually generated FEM meshes for the reductive electrodeposition (left) of a Cu nanoparticle within an aqueous nanodroplet domain or the oxidative stripping (right) of a Cu nanoparticle.

TEM Analysis

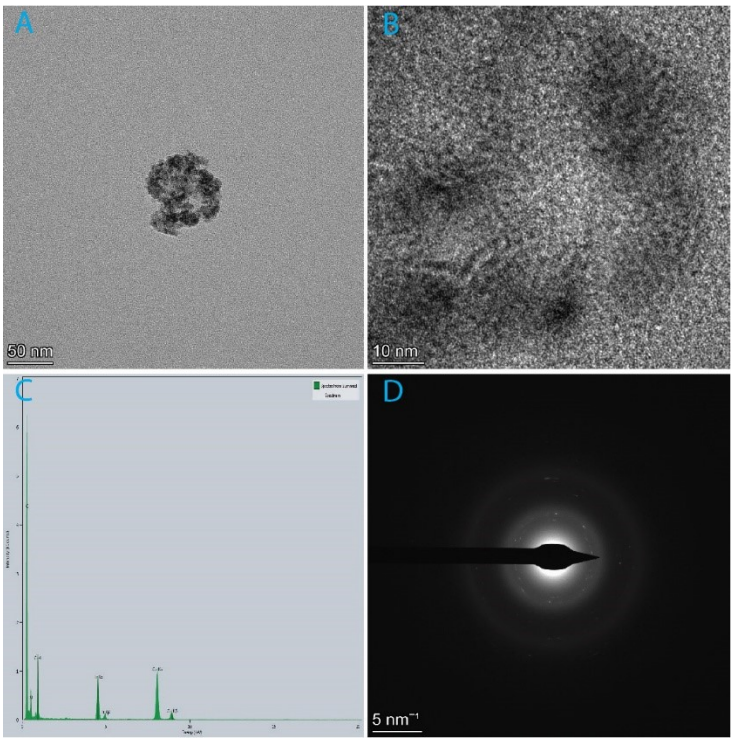

Figure S15 | TEM, EDX, and SAED analysis. A.) TEM image of a copper nanoparticle. B.) High resolution TEM image of a copper nanoparticle. C.) EDX confirming the nanoparticle in A and B is copper. D.) Selected Area Electron Diffraction confirming the nanoparticle is polycrystalline.

References:

1. Glasscott, M. W.; Pendergast, A. D.; Dick, J. E., A Universal Platform for the Electrodeposition of Ligand-Free Metal Nanoparticles from a Water-in-Oil Emulsion System. *ACS Appl. Nano Mater.* **2018,** *1* (10), 5702-5711.
2. Kim, B.-K.; Boika, A.; Kim, J.; Dick, J. E.; Bard, A. J., Characterizing Emulsions by Observation of Single Droplet Collisions—Attoliter Electrochemical Reactors. *J. Amer. Chem. Soc.* **2014,** *136* (13), 4849-4852.